FREQUENCY RESPONSE OF THE SWIM BLADDER AND WEBERIAN OSSICLES OF THE ZEBRAFISH (*Danio rerio*)

An Undergraduate Research Scholars Thesis

by

ANNA MARIE WISNIOWIECKI

Submitted to Honors and Undergraduate Research
Texas A&M University
in partial fulfillment of the requirements for the designation as an

UNDERGRADUATE RESEARCH SCHOLAR

Approved by
Research Advisor: Dr. Brian E. Applegate

May 2015

Major: Biomedical Engineering

TABLE OF CONTENTS

ABSTRACT

Frequency Response of the Swim Bladder and Weberian Ossicles of Zebrafish (*Danio rerio*).
(May 2015)

Anna Wisniowiecki
Department of Biomedical Engineering
Texas A&M University

Research Advisor: Dr. Brian E. Applegate
Department of Biomedical Engineering

In recent years, the use of zebrafish as human disease models has been expanded to include several forms of human deafness. Zebrafish provide convenient hosts for genetic and developmental investigation. However, knowledge of the physical mechanism of zebrafish "hearing" is limited compared to other current models and human physiology. Examining the frequency response of the swim bladder and Weberian ossicles would allow the development of a mechanical understanding of the ear and comparison to the human middle ear. The swim bladder and Weberian ossicles are believed to transmit sound stimuli and give zebrafish the ability to determine an extended frequency range, as "hearing specialists," among fish species. In order to understand the ability of the structures to function as a sound transducer, the frequency response of the structures was measured through phase-sensitive OCT. The anterior swim bladder and Weberian ossicles were visualized via magnitude OCT and data collected along a line through the surface and ROIs. The displacement of the structures in the presence of a sound stimulus suggested coupling of the acoustic energy through the tissue to the anterior swim bladder and to the fourth Weberian ossicle. A tuning response on the anterior swim bladder revealed an increase in vibration magnitude with decreasing frequency stimuli and increasing

sound intensity. *Danio rerio* hears over a range of 100-4000 kHz. However owing to limitations in the current experimental system, we were only able to investigate in the range of 2500-4000 kHz.

ACKNOWLEDGMENTS

First, I would like to thank Dr. Brian E. Applegate for supporting this research as my advisor, and offering his advice, critique, and expertise, including the resources of his lab. I would also like to thank Sangmin Kim, Michael Serafino, Esteban Carbajal, and Dr. Bruce Riley. The former helped make this research possible by constructing and modifying the VOCTV imaging system, which made this study possible, as well as for dedicating time to my tutelage in imaging technology. The latter, Dr. Bruce Riley, contributed both wide expertise and valuable considerations, as well as the specimens themselves. I am indebted to his advice in the subject of this study, which is new to me and little understood.

NOMENCLATURE

dpf	days post fertilization
OCT	optical coherence tomography
PhOCT	phase-sensitive optical coherence tomography
TL	total length
ROI	region of interest

CHAPTER I

INTRODUCTION

Hearing research still contains many questions on vertebrate hearing and deafness mechanisms. Functional relationships between species remain to be clarified. The need for models to support research and development efforts accentuates broadening and applying animal models to find therapies and solutions.

Strides have been made using bioglass and cochlear implants, and in regenerative genetics; however, the sensory maculae of the inner ear are still not well understood in many species, including humans. Cases of hearing loss continue to confound scientists and physicians because of lacking diagnostics and integrated sensory complexity. The molecular environment of the sensory maculae is difficult to study in current model organisms and humans [1]. Causes for the large portion of human deafness conditions are unknown or undiagnosed, and treatments, nonexistent. Significantly, one in six people will experience some form of deafness over their lifetime [2].

Forms of deafness are generally classified as conductive or sensorineural hearing loss. Conductive hearing loss includes physical defects or dampening to the structure of the ear, such as deformed ossicles (bones of the middle ear) or fluid in the transduction space. Sensorineural deafness results from genetic, exposure, aging, or disease related causes and involves nerve-related damage to the inner ear. Some forms of conductive hearing loss can be resolved surgically, while sensorineural forms can take advantage of cochlear implants [3]. In many cases,

available solutions are not cures and knowledge of the causative agent and mechanism are necessary. Hair cell and sensory regeneration is currently a particular focus of research efforts, perhaps a gold standard for deafness therapy, but with a long road ahead. The translation of mechanical to molecular frequency encoding processes is a less understood but vitally important topic to fully understand the causes of and solutions to deafness.

To date, rodents and chickens have made up the majority of research models in the area of human hearing research. Their use can be contributed to the convenient presence of homologous structures, such as a specialized hearing organ, and middle and outer ears [1, 4]. Some drawbacks of these species include reduced developmental accessibility and increased maintenance [1]. In the last thirty years, zebrafish have emerged as a disease model for vascular, neural, genetic, integrative organ and behavioral study [5, 6]. Easy genetic manipulation, low maintenance, transparent embryos, has drawn scientists to increase use of zebrafish in medical research [1].

Zebrafish models provide a convenient platform to launch further studies. Already with multiple mutant lines successfully used to explore deafness [1, 2, 4], the logical step is to see how far the model can be expanded and the analogy of the fish ear to that of the human ear. First, one may note zebrafish have no direct analogue for the middle and outer ear – although parallel structures may be confirmed. *Danio rerio* has no known specialized hearing organ homologous to the cochlea, as well. The important contrast on this point is that zebrafish lack an obvious amplification and selectivity mechanism like that found at the outer hair cells and basilar membrane in humans. However, zebrafish have proven an excellent model for syndromic and

non-syndromic congenital deafness, ototoxic drug-related, and noise-induced hearing loss [2] through the study of similar gene expression, structure-function relationships, transduction paths, and hair cell dynamics, although rudimentary in light of integrated knowledge.

Zebrafish use pressure gradients to perceive sound and are believed to utilize a structure called the Weberian apparatus as a core amplification mechanism to transduce sound [7, 8]. Further, the vibrations are transferred as motion along a mechanically coupled pathway to the sensory organ interface. Then, hair cell activation and a cascade of electrochemical responses elicit the sensation of hearing. Determination of frequency and pitch are encoded through neural projection signaling, and, at a higher level in the brain, origin is computed. The Weberian apparatus consists of interconnected, axially-mobile, vertebrally-derived bones which transmit vibration from the interface of an oscillating air-filled cavity (the anterior swim bladder) to the inner ear itself, on the proximal end. This structure is acclaimed for providing the unique hearing sensitivity for a superorder of fish called Otophysi, which includes *Danio rerio* [7].

The human ear consists of a tympanic membrane which utilizes impedance matching through its relatively large surface area. It provides strong sound wave amplification through translation to a chain of ossicles, relatively tiny bones in the middle ear which are specialized to transduce frequency and sound level with accuracy and safety. Also known as “the hammer”, the stapes footplate is observed articulates angularly with the external cochlea as sound stimuli become more complex [9]. This system of three bones and the enabling tissues and muscles is known for increasing the human hearing range and providing the first step in particular signal determination

and translation. Interestingly, one study on the human ossicles has revealed that potentially damaging resonance can occur at points of the structure within the normal hearing range [10]. Following this mechanical process, the foot plate of the stapes creates pressure waves within the cochlear endolymphatic fluid. The tectorial and basilar membrane, which are over- and under-lying structures to the hearing organ (the Organ of Corti), move relatively in response to fluid waves in the adjacent ducts and cause significant outer hair cell activation at locations of resonance due to gradient mechanical properties at the basilar membrane. Energy is transmitted through the tectorial membrane to the local inner hair cells, causing stimuli amplification and action potentials, corresponding to frequency-place information. The zebrafish is yet to be elucidated in terms of the most important frequency responses along the sound transduction path. Only with this information can the validity of structure-function analogy and use of zebrafish for human research push forward and into the realm of sensory organ therapy and repair.

Although, at first, the auditory path in zebrafish appears different than that of humans, there is much similarity and, with further study, it may be found that function is matched throughout the system, simply in a different package. The zebrafish inner ear consists of seven sensory organs, three of which are axially-differentiated semicircular canals [7, 11]. The form and function of the semicircular canals is conserved to humans. The saccule and utricle sensory organs are the most studied, apart from the semicircular canals. Humans have both an utricle and a saccule; however, both serve solely vestibular functions, detecting linear acceleration in the horizontal and vertical planes, respectively. The utricle lies horizontally in the head and is located next to the semicircular canals. The saccule is oriented vertically and is adjacent to the cochlea. Each of these organs contains an otolithic membrane consisting of otoconia, many small mineralized

crystals, and a gelatinous membrane which couples the mass to the hair cells and increases the inertia in the organ [12]. When one accelerates or tilts their head, the otolithic membrane shifts at a differing pace from particularly the underlying sensory macula, which is home to the hair cell bundles. If the stimulus causes a shift in accordance with the polarity of the central kinocilia, the kinocilia initiates an electrochemical response; otherwise, inhibition occurs.

In zebrafish, the functionality of the utricle is considered to have a similar vestibular mechanism [11]. In contrast, the saccule is referred, in literature, as the main hearing organ [13], even though the same structure-function relationship with respect to the utricle (and the organs in humans) would appear to contradict this. Anatomical orientation and position are basically conserved from the human ear to the zebrafish ear [14]. Both organs in the zebrafish house the macula, directional hair cells, gelatinous membrane, and mineralized mass, respectively, located in order from neural to endolymph-contacting organ faces. The mineralized deposits within each zebrafish ear organ are single, continuous stones with unique geometry [13]. In humans and mice, the saccule has been observed to possess some acoustic sensitivity outside the normal hearing range [15, 16]. This suggests the saccule may have been phased out of an auditory role over the course of evolution. Organ elimination and mutant line studies have produced the conclusion that the saccule is a preferentially auditory organ [17, 18]. The remaining sensory organs are the macula neglecta, an unstudied entity, without an otolith [11], and the lagena, which is thought to play a mixed, secondary auditory and vestibular role [19]. The saccule, lagena, and utricle of both ears are coupled to the vertebral ossicles via a single endolymph-filled canal, called the transverse canal [11]. The transverse canal connects to the lagena and utricle organs indirectly and through narrow openings with the saccule [11]. The saccular-utricular

canal is limited. Endolymph flow completes a pressure wave transducing pathway from the swim bladder (SB) to the sensory macula of the inner ear. A bone shell encases the whole of the inner ear. The physical connections and locations of the zebrafish auditory anatomy, described above, can be viewed in Figure 1. In humans, the sensory cavities are not connected.

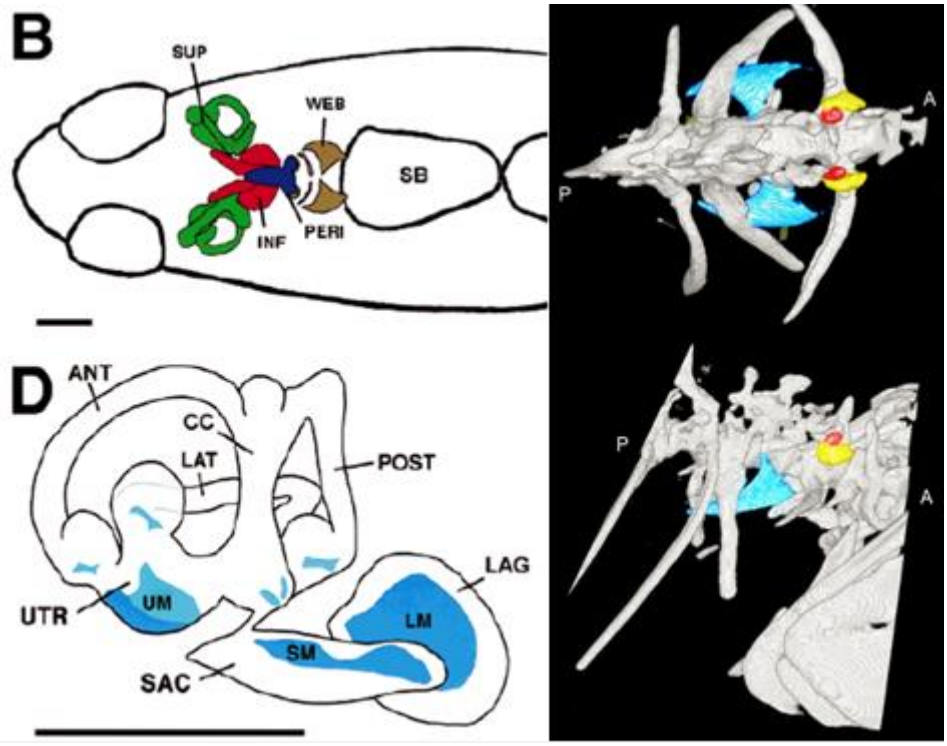

Figure 1. *Danio rerio* auditory chain. **Top left:** Schematic of the auditory chain, dorsal view, highlighting the pars superior (SUP), pars inferior (INF), perilymphatic space (PERI), Weberian ossicles (WEB), and anterior swim bladder (SB). **Bottom left:** Oblique medial view of the right inner ear, showing the utricle (UTR), saccule (SAC), and lagena (LAG). **Top and bottom right:** Micro-CT dorsal and medial views of the Weberian apparatus, showing the tripus in blue, the claustrum in red, and the scaphium in yellow, as well as the precaudal vertebrae, neurals, and paraprophyses. **Top and bottom left:** Pascal I. Bang, et al. The Journal of Comparative Neurology, 438, 173-190, 2001. Scale bars for = 1 mm. **Top and bottom right:** Rebecca Jordan and Dr. Matthew J. Mason, Department of Physiology, Development and Neuroscience, University of Cambridge, http://www.pdn.cam.ac.uk/staff/mason_ma/Popup_Weberian.html.

Frequency selectivity and any source of gain at the saccule have not, thus far, revealed themselves. Some studies on the hearing organs of goldfish, a close relative to the zebrafish, have raised the possibility of tonotopy along the saccular macula in zebrafish by morphological

similarity and hair cell polarity distribution [20]. Similar to the spatial frequency selection in the cochlea, the conclusion saw high frequencies cause hearing loss at the rostral saccule and low frequencies diminish hearing at the caudal end. However, the experiment related to this theory was performed by exposing fish to specific frequency tones for a time period and correlating hair cell loss and damage to location along the length of the organ macula. It is possible this response could also be the result of unknown mechanical dynamics and activation mechanisms. Zebrafish lack an outer/inner hair cell distinction to increase gain, as in the human cochlea. The mechanical properties of saccular hair cells and macula require further study but may utilize specific properties of physical coupling to accomplish frequency selectivity [21, 22]. Understanding these mechanisms may help answer evolutionary questions, as well as transduction techniques across species.

The primary zebrafish sensory organs each contain an aragonite stone called an otolith [2]. In the human ear, the saccule and utricle also contain these inertia-enhancing stones; however, they are formed from calcium carbonate [23]. Both forms of these structures function in the mass loading and transferring of inertial forces to the associated hair cells which are embedded in the otolithic membrane [24]. In zebrafish, tether cells, the original and immotile kinocilium, are also embedded in the otolith itself [25, 26]. Experimentally, otoliths' particular geometric development and size seem to play a role in the facilitation and accuracy of either vestibular or auditory sensing in the end, sensory organs. Defects in otolith development are believed to have a negative effect on the sensitivity of hearing, although only vestibular function studies have been performed [27]. There have been multiple studies providing evidence for tightly regulated otolith development including distinct size and geometry. It is believed that specific proteins and

factors may be produced in a region-specific manner by nearby hair cells, the macula, or the support cells [25]. One study has claimed that, by relocating otoliths between sensory organs, the balance-sensing utricle can sense sound, and, therefore, size could play a differentiating role in separating gravitational and auditory stimuli [17]. The authors note some contradiction in this conclusion since the specimens were 5 dpf. Adult fish have smaller saccular than utricular otoliths [17]. However, if size did play a role, a relative relationship would be required because zebrafish otoliths [28], as well as the rest of the ear, continue to grow over the lifetime of the fish [2, 29]. In addition, sensory specialization as a function of otolith size may prove unreliable when compared to current knowledge of auditory neurological development. Investigations in the Riley lab has observed saccular and utricular neural projections overlapping during development and, later, being eliminated [30].

Zebrafish have been referred to as hearing specialists, a term bestowed on fish species possessing auditory sensitivity-enhancing connections, including the Weberian apparatus, but anatomically found in a variety of configurations [31, 32]. This term only defines these fish as having an adaptation which facilitates a relative increase in frequency detection with respect to normal fish. *Danio rerio* have a hearing range of 100-4000 Hz (several times that of non-specialists). It has been found that zebrafish hearing sensitivity increases from 200 to 4000 Hz with length, coinciding with the development of the Weberian apparatus [33]. This Weberian apparatus, also referred to as Weberian ossicles, is a chain of small axially-arranged bones and ligaments that form a transduction pathway from the swim bladder toward the inner ear for pressure information. These four or five bones (depending on one's source) lie adjacent and connected to the first four spinal vertebrae and are derived from the corresponding neural arches. The neural

arches and parapophyses (also known as transverse processes) are also involved in the system. A symmetric set of these bones lie on each side of the spine and, posteriorly, connect at separate locations on the anterior swim bladder. Changes in pressure cause the swim bladder to inflate, force to be applied to the tripus, and, with the interaction of ligaments and transverse process bones, translation of the intercalarium, scaphium, and, finally, the claustrum. The claustrum articulates with the distal end of the sinus impar (also known as the perilymphatic space). The sinus impar encloses the posterior end of the transverse canal. The vibration and motion of the Weberian ossicles creates indirect fluid pressure waves in the transverse canal. The os suspensorium, an immobile bone attached to the articulating surfaces of the Weberian apparatus on the swim bladder, is sometimes considered the fifth ossicle [34]. The os suspensorium stabilizes the interaction and guides the tripodes into keyhole-shaped holes in the tunica externa membrane of the swim bladder, exposing it to the swelling and shrinking of the swim bladder via the tunica interna [8]. Human ossicles are developmentally derived from the jaw. The developmental origin of the Weberian bones is a point of contention among evolutionary biologists as far as the direct comparison of the human ossicles and the Weberian ossicles. Although zebrafish possess mechanical coupling from swim bladder to inner ear via the transverse canal and Weberian ossicles, many fish have varying degrees of connection between the swim bladder and inner ear [31, 32]. Among fish with a Weberian apparatus, zebrafish have one of the more intimate systems.

Bone composition is another valid parameter when considering differences in the frequency response of the system. Weberian ossicles can be viewed as a direct analog of the human middle ear ossicles. Among fish, Teleost bone composition and development (including the zebrafish) is

most similar to that of humans [29]. Importantly, zebrafish bone contains osteocytes and forms with many of the same tissue types. In contrast, zebrafish bone rarely forms endochondrally, and lacks hematopoietic tissue and similar mechanisms of bone resorption and remodeling. Differing mechanical properties may reveal dissimilar pressure transduction.

The swim bladder, as mentioned previously, refers specifically to the anterior swim bladder. Direct linkage to the so-called auditory chain leads to the assumption of auditory differentiation for the anterior gas bladder. There is also a posterior swim bladder separated from the anterior chamber by a constriction (ductus communicans). The ductus communicans is the repeatable center of gravity in the body [6]. Bladder size is also a function of fish length [6]. It is theorized that the posterior chamber is primarily used to maintain neutral buoyancy while the anterior chamber functions for the purposes of audition [6]. Air volume in the posterior chamber is adjusted by the swallowing and passing of air through a pneumatic duct [6]. Differences in the compliance of the native tissues and respective muscles may be the agent of specialization between the two chambers [35]. Through investigation, removing the swim bladder results in no pressure detection at the inner ear and, therefore, no hearing; however, the hearing bandwidth is not diminished [36]. Furthermore, the addition of high frequency hair cells does not explain the increase in maximum frequency detected [33]. The development of both the swim bladder and the Weberian apparatus can be charged with a clear role in signal amplification and possibly frequency separation. The variation of adaptations creates an obvious division among fish species.

Overall, understanding of the auditory chain in the zebrafish, especially concerning the magnitude and properties of each link in the proposed auditory pathway, is poor and inadequately evidenced. Much has been deduced and presumed from morphological and behavioral studies toward the hearing process of zebrafish. Neurological data and inter-species comparison provide an incomplete understanding and decreased ability to establish a model. Therefore, it is prudent to analyze each native component to elucidate the nature of hearing in zebrafish.

In order to shed light on the physical processing of sound along this pathway, noninvasively observing the motion of the auditory components can add a new perspective and basis for the scientific theories discussed above. A combination of OCT (optical coherence tomography) imaging and vibrometry can accomplish this. By utilizing phase-sensitive OCT (PhOCT) to measure the physical response of structures to a sound stimulus, evidence of functionality can be solidified. This technique provides a high level of anatomical and optical resolution as well as motion and correlated frequency response data. Although previous PhOCT techniques have been limited due to inter-sweep variability and data heavy post-processing, the system utilized here takes advantage of a Vernier-tuned distributed Bragg-reflector laser to remove the synchronization issues caused by moving parts in swept-source methods (which allow fast acquisition) [37]. Increased trigger stability and precise sweep control allows accurate M-scans which are processed to extract phase data with a sensitivity as high as 4 pm positional changes.

The reliability and efficiency of the PhOCT technique utilized in this study has been demonstrated in previous work in this lab [39]. Speed and sensitivity of vibratory measurements

were shown to be comparable to laser Doppler vibrometry. Beyond this, PhOCT greatly broadens our capability to measure previously inaccessible tissues and organs, such as the inner membranes of the cochlea, at both their surfaces and within, in a completely noninvasive procedure. When performing vibration analysis on the tectorial membrane of a mouse, this system was found to have sensitivity as high as several picometers, responding to a barely audible tone at 3 dB SPL. The study presented here also uses the advantage of the noninvasive OCT modality to measure the frequency response, in terms of vibration, as a function of sound frequency and power, within a deficiently explored anatomy. Ultimately, through the characteristics of this technique, the data presented in this paper are representative of the zebrafish specimen as defined in this overall methodology.

Due to the availability of previous studies in multiple species on the frequency response of the middle ear ossicles, the results of the vibrometry study performed henceforth provides the opportunity of comparison of frequency responses, analysis and indirect contrast. The Weberian ossicles and swim bladder are systematically measured and analyzed to observe their frequency response.

CHAPTER II

METHODS

Animal preparation

Wild-type (ABxTL) zebrafish specimen were obtained from the Riley Lab (Texas A&M University, Dept. of Biology). Specimen were sacrificed by overdose with anesthetic (Tricaine) in water, directly prior to conduction of experiments and according to normal protocol. Since the specimen were not living during experimentation and not exclusively euthanized for the purposes of these studies, the Texas A&M University IACUC concluded its approval unnecessary. Each specimen was selected such that its total length (TL) was at least 20 mm, in order to ensure developmental contact of the elements of the Weberian apparatus from ear to anterior swim bladder [38] and inflation of the swim bladders. This method of selection was determined based on previous experiments which show zebrafish length correlates more strongly with development than age [38]. It was not necessary to dissect or alter the body of the specimen in any way. Imaging and sound stimuli were noninvasive. Reported data was collected within 3 hours following specimen sacrifice.

Experimental setup

Each specimen was set in a petri dish, in the groove of a water-soaked sponge, on its side. The imaging laser beam power remained normal to the top, sagittal plane of the specimen to conserve imaging depth and resolution (due to the presence of melanin). The petri dish was attached directly to two translation stages (Thorlabs) and two goniometer (Thorlabs, GNL20) to facilitate specimen rotation in all degrees of freedom and expedite system manipulation. This apparatus

was set into the base of a Zeiss Discovery.V8 microscope that had been modified to allow adjacent OCT imaging, shown in Figure 2. All components were consolidated onto an upright breadboard with sample arm components fed into a sound-dampening enclosure (not shown) surrounding the OCT microscope. Sound-dampening material around four sides reduced room noise from 60 dB to approximately 45 dB.

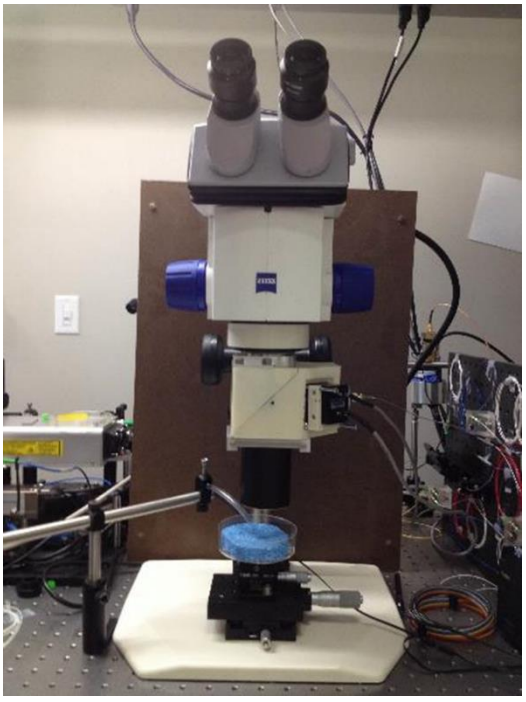

Figure 2. The OCT system incorporated a Zeiss microscope to enable imaging through the same line of sight. A high-quality microphone and speakers were placed close to the ROI of the specimen without disrupting the beam path. The specimen platform consisted of multiple goniometers for adjustment of the specimen and a damp environment.

The OCT system used has been described previously [37, 39], but will be described here, briefly. A 1550 nm center-wavelength, swept-source Vernier-tuned distributed Bragg reflector laser (Insight, 1525-1613 nm, 13mW, sweep rate 44.5 kHz) was connected to an isolator, to prevent back-reflected light from entering the laser cavity, followed by a fused fiber coupler with a splitting ratio of 90:10. The pigtail with 90% of the light was used for the sample arm. The

reference arm contained an attenuator and optical delay line to tune the reference arm power and path length-match the interferometer. The sample arm utilized a circulator to direct light to the sample and then back to the photodetector. The three arms of the circulator (referred to as 1, 2, and 3) directed input sample arm power from 1 to 2, which facilitates flow toward the sample as well as reflected power from the sample, and, then, from 2 to 3. A custom, printed enclosure was attached in line with the microscope, such that the OCT system and microscope used the same objective lens. The second fiber of the circulator fed into the enclosure and was aligned to be produce a vertical beam normal to the sample, via the use of a collimator, right angle mirror, 2-D voice coil mirror (OIM SN3168) and dichroic mirror, and a compound objective lens. The working distance of the combined objectives was 33 mm. The signal of the third fiber of the circulator was passed through polarization paddles to enable the adjustment of the polarization state in the sample arm to match that in the reference arm in order to maximize the signal to noise ratio. The signal from the polarization paddles was recombined with the reference arm by a 50:50 FC coupler, creating interference. Finally, the recombined signal met with a balanced photodetector (Thorlabs, PDB460C) to give the spectral interferogram, which is used construct the complex A-line, or depth-resolved reflectivity profile. Balanced photodetection uses low frequency feedback to cancel common mode noise and provides amplification of differences between multiple paths. LabVIEW control of the voice coil mirror allowed x and y scanning of the specimen and was used to compile volumes. Vibration profiles were collected by aligning the location of interest in x and y to the central reference of the voice coil mirror and acquiring the complex reflection over time at depths within the focal plane range. Processing was continuously transferred to the FPGA (field-programmable gate array) to enable real-time data collection and display. Spectral interferograms are measured coincident with tonal sound stimulation to get

p(k,t), where k is spatial frequency (or wavenumber) and t is time. An inverse Fourier transform is calculated along k to yield P(z,t), where z is the axial spatial dimension. The magnitude of P(z,t) is the a set of A-lines measured as a function of time. If the phase of P(z,t) is extracted and the Fourier transform calculated along t, the result is the complex signal dz(z,f), where f is frequency. The magnitude of dz(z,f) is the amplitude of the motion due to the sound stimulation. The phase of dz(z,f) is the phase of the motion relative to the sound stimulation. The schematic for the OCT system is shown in Figure 3.

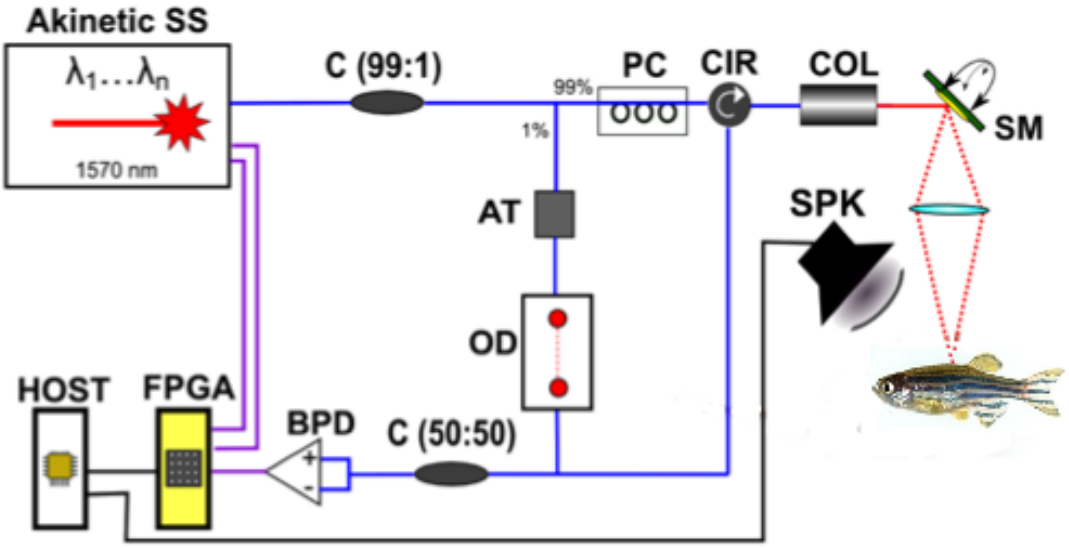

Figure 3. Schematic of the swept-source OCT system implemented to conduct PhOCT.

The best hearing range of *Danio rerio* lies with relatively lower frequencies and is subject to environmental and electronic low-frequency noise. To increase the fidelity of these measurements, a sound suppressing enclosure was erected about the sample. Swept-source lasers have a long coherence length which enhances signal roll-off. The use of a balanced detector suppresses common mode noise. In order to conduct vibrometry, phase data is extracted from the

signal and converted, by the previously mentioned relation, to physical displacement [40]. The phase-stable nature of the laser used in this experiment eliminated the issue of inherent phase jitter found in many swept-laser sources. During volume vibrometry data sets (4D), the high data influx creates the need to re-distribute the computing load by transferring processing to a field-programmable gate array (FPGA), following the digitizer. This allows the results of *in vivo* experiments to be displayed in real-time. Dead zebrafish specimen were chosen for this experiment due to the increased experimental complexity presented by an aqueous environment. However, this is a pilot study that, if successful, will be followed by *in vivo* experiments, designed to conserve full physiological functionality and underwater stimulus and response monitoring fidelity. As the zebrafish is imaged promptly after sacrifice, passive mechanics should be measurable and conserved.

OCT can be used to conduct vibrometry by analyzing the phase component of the reflected OCT signal (PhOCT). Small changes in the position of the specimen anatomy, which are essentially reflectors, result in a phase change of the signal over time. The Fourier transform of the phase gives the distribution of the frequency content at each point/location in the A-line, per time point, in the case of an m-scan, where the fourth dimension is time. Therefore, the phase of the signal represents the displacement of each location due to each frequency. Displacement and phase are related according to Equation 1

$$\delta z=\lambda_0/4\pi n*\delta\phi \qquad (1),$$

where z is displacement in nm, λ_0 is the center wavelength in nm of the laser source, and ϕ is the phase in degrees. Phase sensitivity is a function of the phase noise and, therefore, it is important to minimize background room and electronic noise. This form of vibrometry could be considered

an internal measurement compared to standard laser Doppler vibrometers which measure only movement of the surface. PhOCT enables the measurement of motion along the entire line image (A-line). With the addition of PhOCT, OCT can be utilized as a functional as well as anatomical modality.

A dispersion correction factor was collected before data collection begun for each specimen. Dispersion is the dependence of a material's refractive index on light frequency, in optics, and causes chromatic aberration in lenses. The goal of dispersion correction is to numerically compensate for the dispersion mismatch between the arms of the interferometer. If left uncorrected, the axial resolution of the imaging system would be severely degraded. In the shot-noise limit, the SNR should be 110 dB. SNR was measured to be ~106 dB. A LabVIEW control program was used to collect and apply the dispersion correction and background subtraction as part of the OCT and vibrometry data collection, processing, and display.

Prior to making vibrometry measurements, a sound calibration was performed with the speaker using a precision microphone (LinearX Systems, M53) by varying the input voltage. Volume level (dB SPL) was verified with a sound meter. Sound stimuli were triggered by a function generator, sent through a DAQ (NI USB-6211) and amplifier, and carried through an earbud speaker (ClarityOne) followed by tubing, to a location near the region of interest (ROI). The data collection software was coded in LabVIEW. Further data processing was performed in MATLAB.

Application of OCT for vibrometry

OCT B-scan images were captured initially to localize the anatomy of interest. OCT volume images are also presented to add to overall understanding of zebrafish anatomy via OCT. Because OCT has not been a conventional method to probe zebrafish anatomy thus far, the first important task involved identifying the anatomy of the zebrafish in the light of the modality. Volumetric anatomical data collected from head to mid-body allowed for location of structures based on "land-marking" the eyes, semicircular canals, and anterior swim bladder, in particular. These structures were easily identified due to the characteristic of highly reflective fluid-solid interfaces which produce strong image contrast due to differences in density and refractive index. The anterior swim bladder was found by scanning toward the tail from the head until the characteristic large, air-filled cavity was revealed, following a transition of the spinal column anatomy beyond the precaudal vertebrae. The fourth Weberian ossicle required meticulous comparison to reported functional theories due to the presence of several sets of functionally-separated bones initiating along the precaudal vertebrae. Specifically, the tripus was elucidated from the region of the precaudal vertebrae. Its identification was aided by the presence of the fourth (precaudal) rib which originates near the top of the fourth vertebra, while the tripus spurs from the bottom of the same vertebra (viewed laterally).

Specific A-lines containing pixels representing the near membrane of the anterior swim bladder or bone structure of the Weberian ossicles were centered within the voice coil mirror scanning range and targeted for the collection of the vibratory response. Pure tones were played in the direction of the targeted structure while complex OCT data was simultaneously acquired. A-lines constructed from the OCT magnitude were used to select the appropriate depth to extract the

phase change at ROI point locations. Pixels in the A-line were selected and measured to quantify the response of anatomical ROIs, converting its complex phase to a measure of magnitude and phase of anatomic displacement in response to the tone. Line rate reduction of one was applied during collection of these m-scans, essentially throwing out every other line, so that the scan would not outpace the response time of the voice coil mirror.

A study of peripheral auditory structures by Higgs et al. provides evidence that zebrafish of TL 20 mm detect the full hearing range of the species, up to 4000 Hz [38]. This ensures the prediction of stimuli eliciting best frequency tuning and detection between 800 and 1000 Hz as reasonable [33]. However, due to low frequency noise from system components, 2500, 3000, 3500, and 4000 Hz were used for interrogation in this initial "proof of concept/structure-function relationship" experiment. Frequencies in this range were applied and phase was analyzed for evidence of tuning (signal handling) in addition to differential tissue displacement toward the conclusions of this study.

M-scans at 2500 Hz were collected in an A-line containing the anterior swim bladder membrane/gaseous interface and through the tripus. These data sets were used to show the general frequency response of the tissues in the A-line, particularly the tripus due to difficulty in its identification. For this reason, only data describing the tuning response of the anterior swim bladder was collected. In the analysis of the anterior swim bladder, m-scans with stimuli varying from 2.5-4 kHz in frequency and 50-80 dB SPL in volume were collected. The speaker response in the above ranges was verified and found to reliably produce the fundamental frequencies with small, secondary harmonic expression. However, the speaker response at 3 kHz showed a larger

harmonic than by the other stimulus frequencies, valuing only 15 dB SPL less than the fundamental frequency amplitude. Each vibrometry data set was taken from multiples of the indicated measurements to display the maximal and most faithful representation from a single, sacrificed zebrafish specimen within three hours of death. Since this study is preliminary, a greater quantity of specimen will be imaged in the following these experiments to verify repeatability of results.

Data analysis

Post-processing of magnitude OCT images and m-scans representing the anterior (auditory) swim bladder and the ossicular chain (tripus, the fourth Weberian ossicle) was performed in MATLAB. Normal OCT processing was performed continuously during data collection. Additional filtering, contrast, and color map manipulation were applied for magnitude OCT data to sharpen anatomic features and for ease of viewing. These images were used to locate and qualify the anatomy represented in vibrometry data. M-scan data of the anterior swim bladder was combined to create a tuning curve, relating input frequency to vibratory displacement in the presence of a stimulus for each sound intensity. The noise floor was defined by the mean of the vibration magnitude at frequencies away from the stimulus and above the low frequency system noise for each m-scan. Comparison to the mean phase noise plus three times the standard deviation was used as a cutoff, i.e. signals smaller than this were not considered in the analysis. The noise distribution for signals at or above this level should be approximately normal and therefore unbiased [41]. Correlation was also performed between anatomic points from the same origin (SB or tripus). M-scan translation from signal phase to displacement along with noise reduction processing was performed in MATLAB. Vibrometry phase and magnitude were

graphed to observe the differential frequency response. The magnitude data was processed as described above and phase data was averaged over the pixel locations representing the ROI since the structures should move as one piece. All vibrometry data sets were referenced to surrounding tissue to judge functional movement as well.

CHAPTER III

RESULTS & DISCUSSION

Results

In this nearly real-time OCT system, volumetric image data around the structure of interest was captured based on a B-scan containing the structure of interest. 3-D views of the volumetric data, displayed in Figure 4 and Figure 5, further confirm the shape of the cavity of the swim bladder and parallel structures in the plane of the lateral cross-section through the center of the tripus. The structures of interest, the swim bladder and tripus, were identified based on visualization and concluded as the desired targets based on relative motion characteristic.

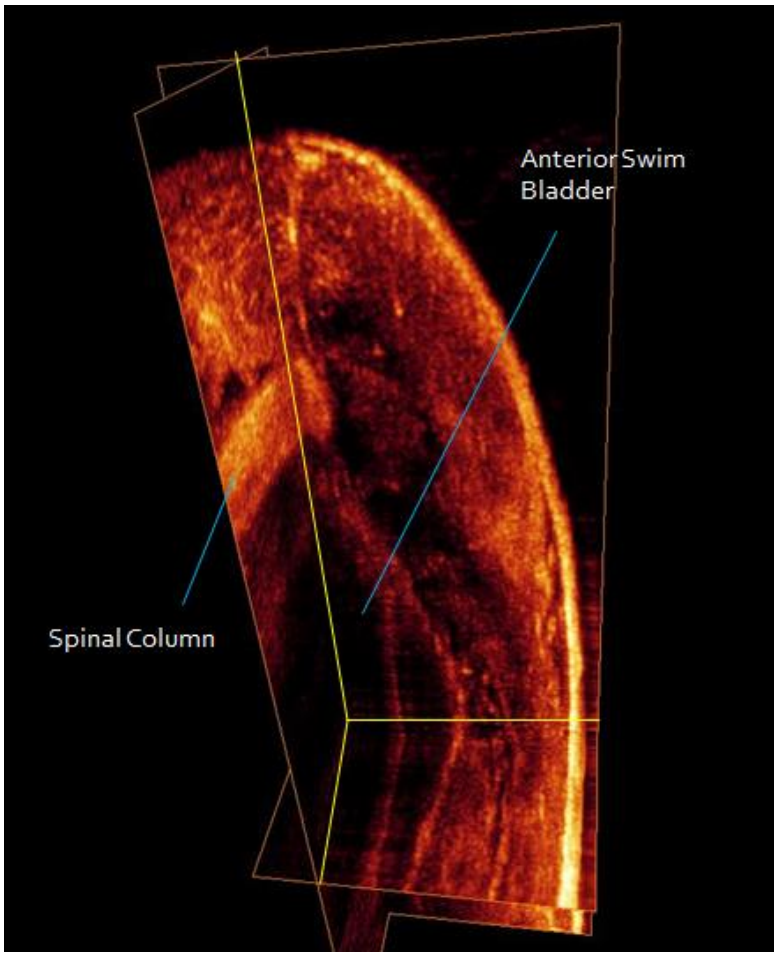

Figure 4. Coordinate plane cross-sections of a magnitude OCT volume containing the anterior swim bladder.

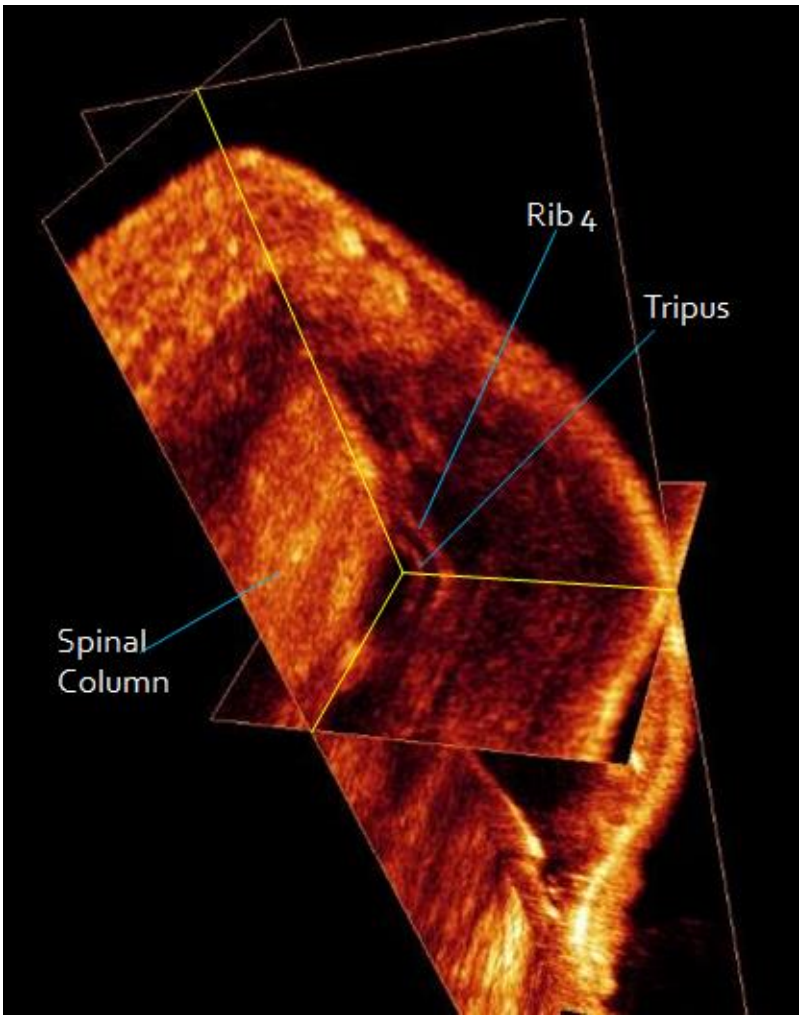

Figure 5. Coordinate plane cross-sections of a magnitude OCT volume containing the tripus, fourth, precaudal rib and spinal column.

1-D vibrometry data taken over an A-line revealed the transmission of acoustic energy to the swim bladder (through overlying tissue) and the presence of relative motion at the tripus in the company of an applied, 2500 Hz stimulus. Data associated to the positions of the nearest anterior swim bladder membrane, tissue between the top membrane and fish skin/surface, and the surface itself are displayed in Figure 6. The surface and tissue preceding the near anterior swim bladder membrane measured displacement of 2.77±0.142 nm and 3.58±0.310 nm at 2500 Hz,

respectively. At the near ASB membrane, displacement rose to its maximum value in the A-line of 3.86±0.0983 nm.

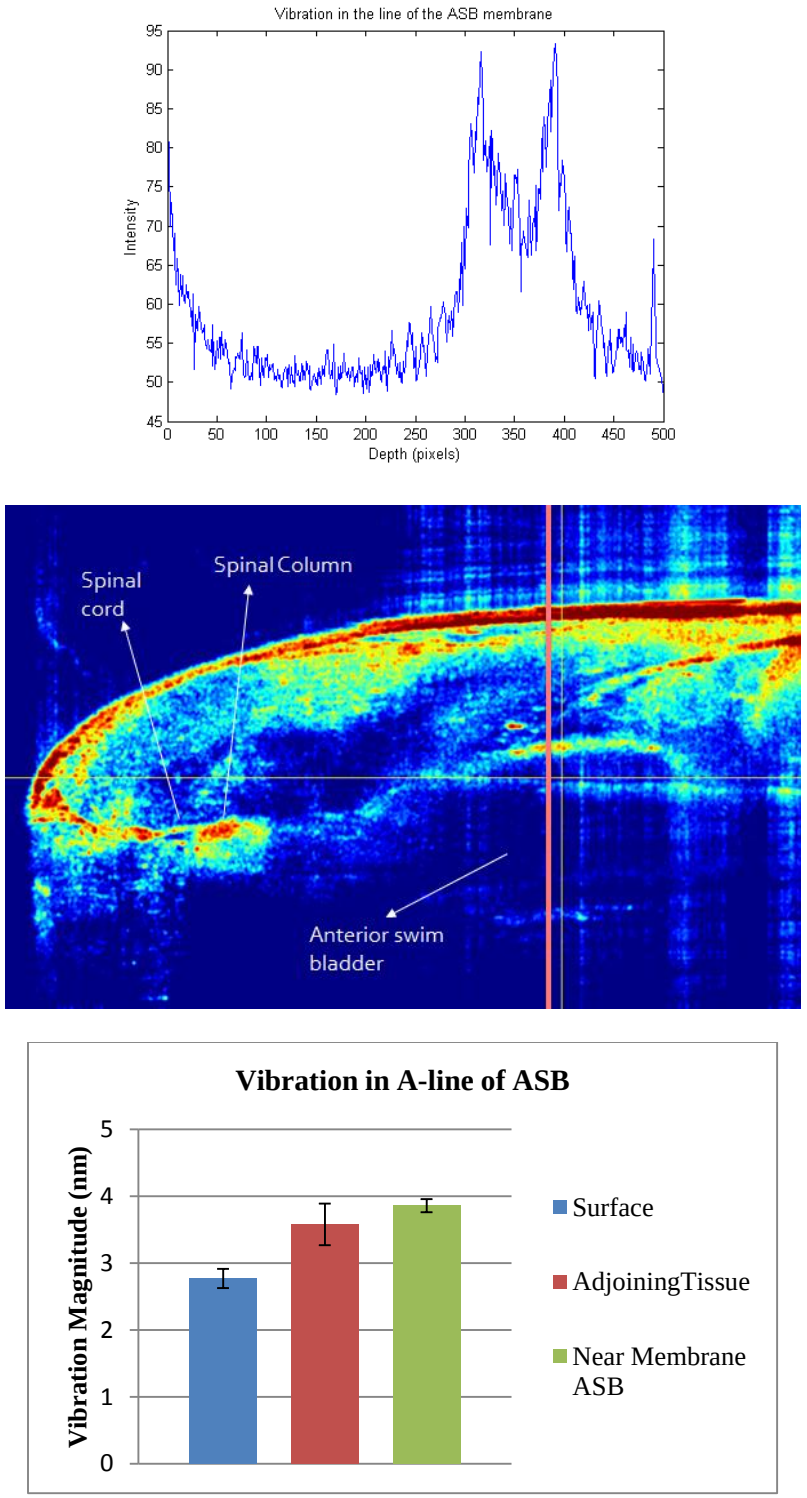

Figure 6. Frequency response at the anterior swim bladder; **Top:** B-scan through ASB. Pink line indicates position of the A-line. **Middle:** OCT A-line along the A-line versus vibration magnitude at 2500 Hz. **Bottom:** Comparison of extracted, 2500 Hz vibration magnitude at the surface interface, tissue lying between the surface and ASB membrane, and ASB membrane. Valid motion determined against the noise mean plus three standard deviations.

The structures inferred to be the tripus, fourth precaudal rib, and surface in the same specimen were interrogated and their frequency responses analyzed. The response at 2500 Hz revealed vibration magnitude of 3.56±0.961 nm, 1.21±0.145 nm, and 1.19±0.110 nm at these locations, respectively, in the A-line. The specimen was 20 mm TL. OCT magnitude volumes used to isolate the ROIs are shown in Figure 7.

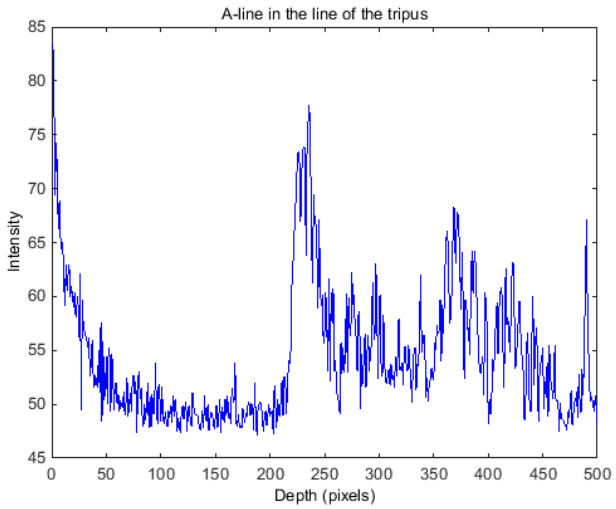

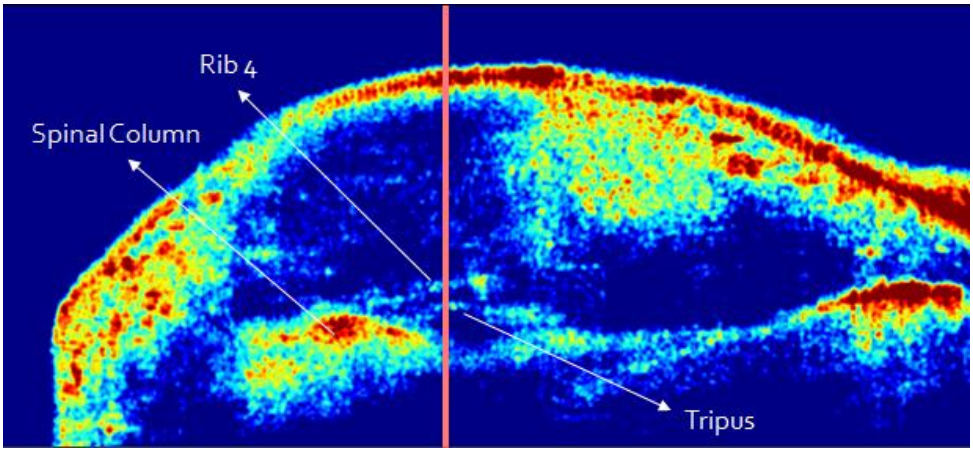

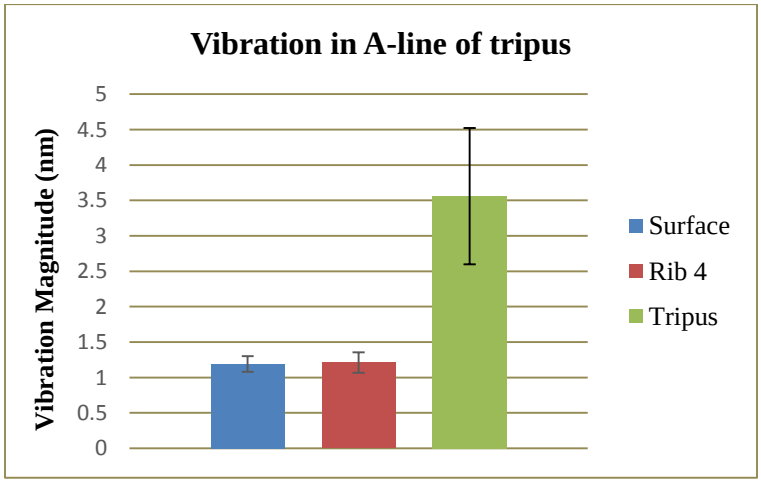

Figure 7. Frequency response at the fourth Weberian ossicle; **Top:** B-scan through the tripus. Pink line indicates position of the A-line. **Middle:** OCT A-line along the A-line versus vibration magnitude at 2500 Hz (masked based on A-line magnitude). **Bottom:** Comparison of extracted, 2500 Hz vibration magnitude at the surface interface, fourth, precaudal rib, and fourth Weberian ossicle, the tripus. Valid motion determined against the noise mean plus three standard deviations.

A 33 mm TL specimen was measured to obtain the tuning response of the anterior swim bladder membrane. The frequency response at 2500, 3000, 3500, and 4000 Hz at 50, 60, 70 and 80 dB SPL is displayed as a function of sound intensity and frequency in Figure 8a and 8b. Figure 8a shows the trend of lower displacement with lower sound pressure level, excepting the behavior at 3 kHz. Motion at 3 kHz, 60 dB SPL was not determined to be significant. Figure 8b shows that greater vibration magnitude corresponds to frequencies closer to the "best" frequency (greater displacement at 2500 Hz).

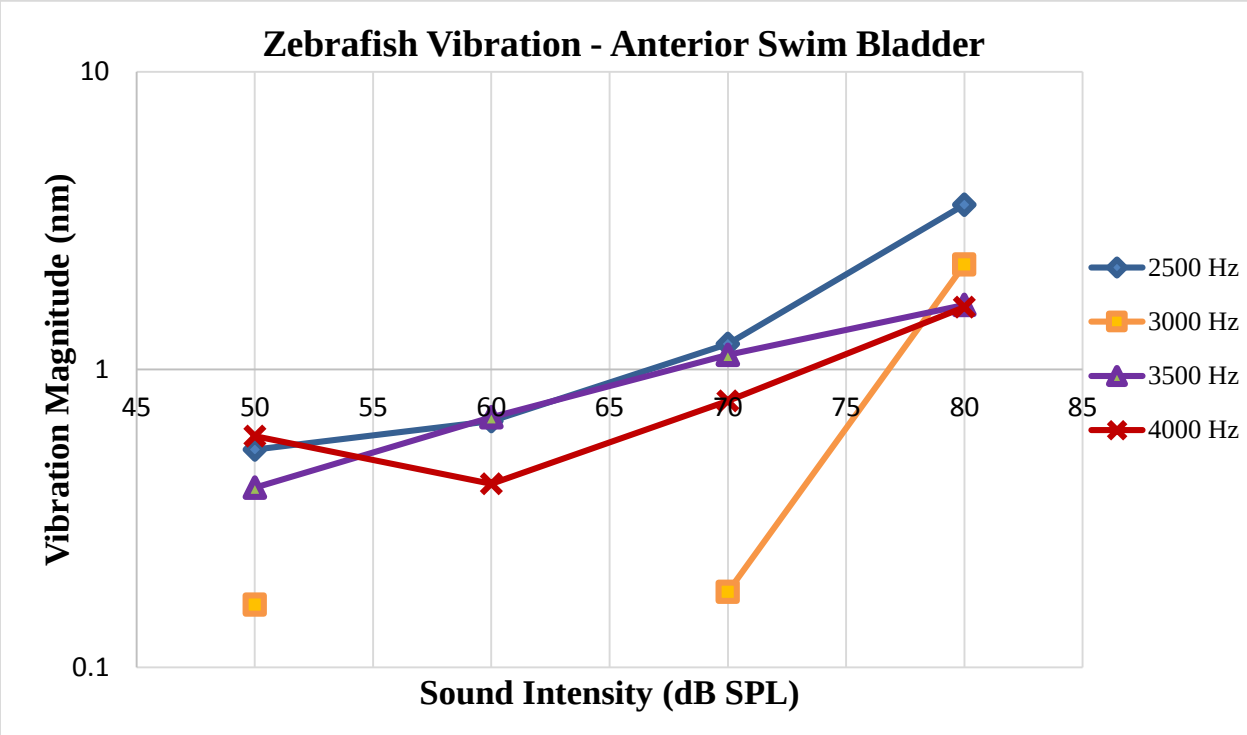

(a)

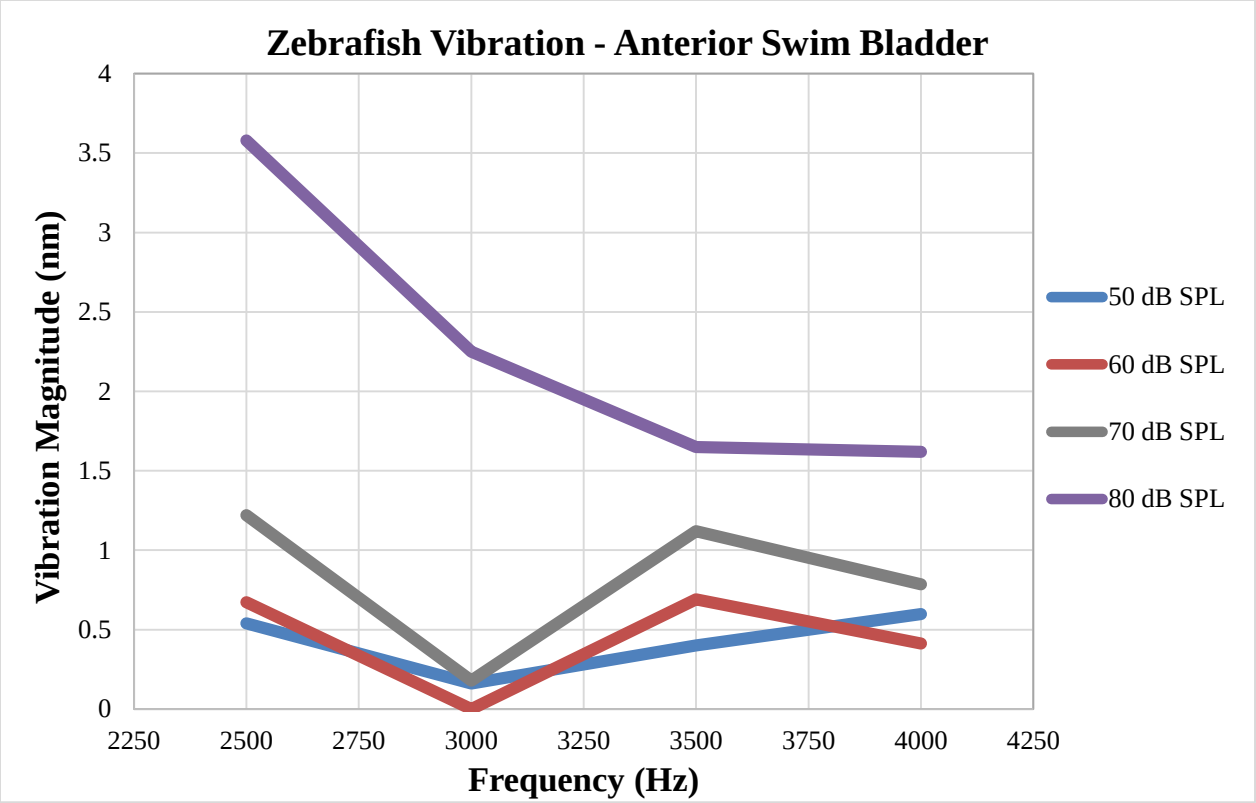

(b)

Figure 8. Vibration magnitudes of *ex vivo* zebrafish anterior swim bladder as a function of **(a)** sound intensity and **(b)** stimulus frequency.

Discussion

OCT magnitude volumes presented above represent the ability to explore the zebrafish anatomy with OCT. The ability to identify and localize the more variable and small components of the auditory system continues to represent a challenge. A difference in the anatomical presentation among specimen was seen, especially when attempting the identification of the ossicular (and other precaudal spur) bones as well as the hearing sensory organs. This may be due to larger deviation in development than was expected or developmental integration with adjacent organ systems. Although the tripus, precaudal 4th rib, os suspensorium, and several sensory organs were found in individual specimen, consistent recognition was not achieved due to lack of

“landmarks.” The posterior and anterior swim bladder, spinal column, and semicircular canals were observed dependably although varying in geometric parameters and, in some cases, containing additional tissue.

Data collected through an A-line containing the swim bladder was consistent with characteristics expected for an auditory-serving organ akin to a human tympanic membrane. In order from tissue external to the specimen to the most internal, near membrane of the anterior swim bladder, 2500 Hz stimuli produced significant responses at the surface, near membrane, and the tissues between. Frequency content at these sites had strong singularity at 2500 Hz. It can be inferred that the faithful signal transmission through tissue surrounding an auditory organ is expected and corresponds to the evolutionary adaptation associated with advanced hearing in *Danio rerio*. This suggests that the anterior swim bladder aids in the delivery of acoustic energy into the internal tissues. One conclusion drawn from the overall frequency response in the line of the anterior swim bladder is that the gas bladder should indeed experience a pressure change, as previously hypothesized, on the arrival of a stimulus. Interestingly, the vibration magnitude at the near membrane of the ASB is larger than that observed at the surface and adjacent tissues. This may suggest a structural arrangement of anatomy leading inward to the ASB membrane which lends itself to the enhancement of the auditory system.

The function of the tympanic membrane is to transmit the auditory energy of a signal to the ossicular chain with fidelity. Therefore, the frequency response in the line of the tripus was observed next. Relative motion in the A-line was dominated at the location of the tripus with a displacement of 3.56 nm, larger than at other sites of interest. The response seen at the surface

interface followed up with displacement of 1.19 nm motion and, at the site of the fourth precaudal rib, a 1.21 nm displacement was observed. Areas of no signal between the surface and spinal column lead to the conclusion that significant differential motion is seen at the tripus. Also, due to negligible material interface with the stimulus itself, the tripus and rib must vibrate in response to the nearest stimulated structure, the anterior swim bladder, or possibly through another path through the inner ear, to which it has direct attachment, on either the anterior or posterior end. The direction of motion measured is parallel to the incident light, and, therefore, describes motion either laterally or medially. This finding suggests the functional ability of the Weberian apparatus to move differentially with respect to the spinal axis uniquely against other spinal column-spurring bone systems, such as the ribs, and, likely, also, the neurals. 2500 Hz motion at the surface is expected since the stimulus travels through a single medium, making the variation of wavelength unlikely. The human ossicular chain (middle ear) responds to a stimulus by faithful frequency transmission at its cochlear interface. Further study is required to reveal the full mechanisms and frequency response of the zebrafish ossicular components.

Tuning curve data for the ASB suggests a linear relationship between vibration magnitude and sound intensity (excluding the anomaly at 3 kHz). This result is similar to that seen in the mammalian middle and outer ear, including the human ear. A linear relationship suggests the hearing components do not provide gain. A decrease in vibration magnitude is seen as frequency increases which may be expected as the frequency of the stimulus is removed farther from the frequency of best hearing (800-1000 Hz). Examining stimulus sound intensity versus vibration magnitude, excepting 50 dB SPL, which is close to room noise, the displacement seen increases with sound intensity. At 3 kHz, however, there is a definite deviation from any predictable

pattern for 50-70 dB SPL. This cannot be completely attributed to a speaker error at 3 kHz since the speaker response was verified and the other stimulus frequencies provided significant proof of transmission to the ROIs. Looking more closely at the 3 kHz response, the displacement at the harmonic frequency, 6 kHz, was greater than that at 3 kHz, except at 80 dB SPL. Therefore, the lack of significant measured displacement, which appears to instead be shifted to the second harmonic, may be a characteristic of the ASB frequency response. This response could portray a complex filtering or frequency determination method, a safety mechanism employed some place along the auditory chain, or an acute experimental error.

CHAPTER IV

CONCLUSIONS

In this preliminary study, physical evidence was obtained supporting the functional theory of the hearing system of *Danio rerio*, a fish categorized as a hearing specialist among fish species. Sound-evoked motion in the anterior swim bladder and the Weberian apparatus was measured using PhOCT. The frequency response of the anterior swim bladder and tripus, a component in the Weberian ossicular chain, specifically showed the transmission of an auditory stimulus at 2500 Hz to the membrane the anterior swim bladder and a relative response at the posterior end of the Weberian apparatus (at the tripus). The frequency response is outlined with the "enabling" stimulus as a causative agent of differential motion of the auditory chain, where the stimulus frequency is found within the specimen adult hearing range. Looking at vibration magnitude as a function of frequency and sound intensity, frequencies closer to that of best zebrafish hearing and larger sound intensities produced larger vibration magnitudes, except at 3000 Hz. The deviant response to a 3000 Hz sound stimulus was unexpected. Further frequency interrogation at a wider range of frequencies and with more comprehensive measurement of the individual auditory components is necessary to confirm the frequency response seen. Overall, the data suggests that the acoustic energy is indeed traveling along the predicted pathway. Moreover, the data obtained herein does not conflict with the analogy to the human outer and middle ear and requires and promotes further and more complete characterization of the swim bladder and Weberian apparatus to build a solid foundation for inner ear characterization and physical disease comparisons. This work encompasses the first, completely noninvasive, PhOCT mechanical measurements of the zebrafish hearing system.

REFERENCES

1. T. T. Whitfield, P. Mburu, R. E. Hardisty-Hughes, and S. D. M. Brown, "Models of congenital deafness: Mouse and zebrafish " Drug Discovery Today: Disease Models **2**, 85-92 (2005).

2. S. Baxendale and T. T. Whitfield, "Zebrafish Inner Ear Development and Function," in Development of Auditory and Vestibular Systems, R. Romand and I. Varela-Nieto, eds. (Academic Press, 2014), pp. 64-97.

3. Hearing Loss Association of America "Types, Causes and Treatment," http://www.hearingloss.org/content/types-causes-and-treatment.

4. D. M. Fekete, "Development of the vertebrate ear: insights from knockouts and mutants," Trends Neurosci. **22**, 263-269 (1999).

5. A. Miklosi and R. J. Andrew, "The Zebrafish as a Model for Behavioral Studies," Zebrafish **3**, 227-234 (2006).

6. G. N. Robertson and B. W. Lindsey, "The contribution of the swim bladder to buoyancy of the adult zebrafish: a morphometric analysis," Journal of Morphology **269**, 666-673 (2008).

7. P. I. Bang, W. F. Sewell, and J. J. Malicki, "Morphology and cell type heterogeneities of the inner ear epithelia in adult and juvenile zebrafish (*Danio rerio*)," J. Comp. Neurol. **438**, 173-190 (2001).

8. N. C. Bird and L. P. Hernandez, "Morphological variation in the Weberian apparatus of Cypriniformes," Journal of Morphology **268**, 739-757 (2007).

9. A. M. Huber and A. Eiber, "Vibration properties of the ossicle and cochlea and their importance for our hearing system," HNO **59**, 255-260 (2011).

10. C. -F. Chou, J. -F. Yu, and C. -K. Chen, "The natural vibration characteristics of the human ossicles," Chang Gung Medical Journal **34**, 160-165 (2011).

11. M. M. Bever and D. M. Fekete, "Atlas of the developing inner ear in zebrafish," Developmental Dynamics **223**, 536-543 (2002).

12. I. Hughes, I. Thalmann, R. Thalmann, and D. M. Ornitz, "Mixing model systems: Using zebrafish and mouse inner ear mutants and other organ systems to unravel the mystery of otoconial development," Brain Res. **1091**, 58-74 (2006).

13. T. T. Whitfield, B. B. Riley, M. Chiang, and B. Phillips, "Development of the zebrafish inner ear," Developmental Dynamics **223**, 427-458 (2002).

14. C. Platt, "Zebrafish inner ear sensory surfaces are similar to those in goldfish," Hear. Res. **65**, 133-140 (1993).

15. G. P. Jones, V. A. Lukashkina, I. J. Russell, and A. N. Lukashkin, "The Vestibular System Mediates Sensation of Low-Frequency Sounds in Mice," Journal of the Association for Research in Otolaryngology **11**, 725-732 (2010).

16. K. Sheykholeslami and K. Kaga, "The otolithic organ as a receptor of vestibular hearing revealed by vestibular-evoked myogenic potentials in patients with inner ear anomalies," Hear. Res. **165**, 62-67 (2002).

17. M. Inoue, M. Tanimoto, and Y. Oda, "The role of ear stone size in hair cell acoustic sensory transduction," Sci. Rep. **3**, 2114 (2013).

18. B. B. Riley and S. J. Moorman, "Development of utricular otoliths, but not saccular otoliths, is necessary for vestibular function and survival in zebrafish," Journal of Neurobiology **43**, 329-337 (2000).

19. M. Haden, R. Einarsson, and B. Yazejian, "Patch clamp recordings of hair cells isolated from zebrafish auditory and vestibular end organs," Neuroscience **248**, 79-87 (2013).

20. M. E. Smith, J. B. Schuck, R. R. Gilley, and B. D. Rogers, "Structural and functional effects of acoustic exposure in goldfish: evidence for tonotopy in the teleost saccule," BMC Neuroscience **12**, 19 (2011).

21. R. R. Fay and A. N. Popper, "Evolution of hearing in vertebrates: the inner ears and processing," Hear. Res. **149**, 1-10 (2000).

22. K. –H. Ahn, "Enhanced signal-to-noise ratios in frog hearing can be achieved through amplitude death," Journal of The Royal Society Interface **10**, 20130525 (2013).

23. C. Sollner and T. Nicolson, "The Zebrafish as a Genetic Model to Study Otolith Formation," in Biomineralization: Progress in Biology, Molecular Biology, and Application, E. Bauerlein, ed. (John Wiley & Sons, 2006), pp. 229-243.

24. L. Abbas and T. T. Whitfield, "4 - The zebrafish inner ear," Fish Physiology **29**, 123-171 (2010).

25. G. A. Stooke-Vaughan, P. Huang, K. L. Hammond, A. F. Schier, and T. T. Whitfield, "The role of hair cells, cilia and ciliary motility in otolith formation in the zebrafish otic vesicle," Development **139**, 1777-1787 (2012).

26. M. Tanimoto, Y. Ota, M. Inoue, and Y. Oda, "Origin of inner ear hair cells: morphological and functional differentiation from ciliary cells into hair cells in zebrafish inner ear," J. Neurosci. **31**, 3784-3794 (2011).

27. D. M. Fekete, "Developmental biology. Rocks that roll zebrafish," Science **302**, 241-242 (2003).

28. D. V. Lychakov and Y. T. Rebane, "Otolith regularities," Hear. Res. **143**, 83-102 (2000).

29. A. Apschner, S. Schulte-Merker, and P. E. Witten, "Chapter 10 - Not All Bones are Created Equal – Using Zebrafish and Other Teleost Species in Osteogenesis Research," Methods Cell Biol. **105**, 239-255 (2011).

30. B. B. Riley, Department of Biology, Texas A&M University, College Station, TX 77843 (personal communication, 2014).

31. X. Deng, H. J. Wagner, and A. N. Popper, "The Inner Ear and its Coupling to the Swim Bladder in the Deep-Sea Fish *Antimora rostrata* (Teleostei: Moridae)," Deep Sea Res. Part 1. Oceanogr. Res. Pap. **58**, 27-37 (2011).

32. A. N. Popper and R. R. Fay, "Rethinking sound detection by fishes," Hear. Res. **273**, 25-36 (2011).

33. D. M. Higgs, A. K. Rollo, M. J. Souza, and A. N. Popper, "Development of form and function in peripheral auditory structures of the zebrafish (*Danio rerio*)," J. Acoust. Soc. Am. **113**, 1145-1154 (2003).

34. T. GRANDE and B. YOUNG, "The ontogeny and homology of the Weberian apparatus in the zebrafish *Danio rerio* (Ostariophysi: Cypriniformes)," Zool. J. Linn. Soc. **140**, 241-254 (2004).

35. B. W. Lindsey, F. M. Smith, and R. P. Croll, "From inflation to flotation: contribution of the swimbladder to whole-body density and swimming depth development of the zebrafish (*Danio rerio*)," Zebrafish **7**, 85-96 (2010).

36. D. G. Zeddies, "Development of the acoustically evoked behavioral response in zebrafish to pure tones," J. Exp. Biol. **208**, 1363-1372 (2005).

37. J. Park, E. F. Carbajal, X. Chen, J. S. Oghalai, and B. E. Applegate, "Phase-sensitive optical coherence tomography using an Vernier-tuned distributed Bragg reflector swept laser in the mouse middle ear," Opt. Lett. **39**, 6233-6236 (2014).

38. D. M. Higgs, M. J. Souza, H. R. Wilkins, J. C. Presson, and A. N. Popper, "Age- and Size-Related Changes in the Inner Ear and Hearing Ability of the Adult Zebrafish (Danio rerio) " JARO - Journal of the Association for Research in Otolaryngology **3**, 174-184 (2002).

39. H. Y. Lee, P. D. Raphael, J. Park, A. K. Ellerbee, B. E. Applegate, and J. S. Oghalai, "Traveling wave propagation measured within tissue using volumetric optical coherence tomography vibrometry," (2014).

40. S. S. Gao, P. D. Raphael, R. Wang, J. Park, A. Xia, B. E. Applegate, and J. S. Oghalai, "In vivo vibrometry inside the apex of the mouse cochlea using spectral domain optical coherence tomography " Biomedical Optics Express **4**, 230 (2013).

41. H. Gudbjartsson and S. Patz, "The Rician Distribution of Noisy MRI Data" Magnetic Resonance in Medicine **34,** 910-914 (1995).